



## Article

# Heat Production from Single Fracture Hot Dry Rock, Applications for EGS Reservoir Design

Zheng Su \* and Haizhen Zhai

Guangzhou Institute of Energy Conversion, Chinese Academy of Sciences, Guangzhou 510640, China; zhaihz@ms.giec.ac.cn

\* Correspondence: suzheng@ms.giec.ac.cn

**Abstract:** A new analytical solution for the thermal-hydraulic coupling process is derived with a 1-D steady state conductive heat flow in the body of hot rock with perpendicular water flow in the single fracture and transient heat transfer from rock to water. The heat produced from the hot rock via water flow in the idealized single fracture is demonstrated by arithmetic equations. The applicability of the analytical solution is verified by numerical calculations and is limited to conditions with fast water flow rates or high water flux and long fluid pathways. The lifetime of an EGS reservoir in these reference conditions is 23.2 years and is confined by the produced water temperature of 150 °C for commercial utilization. The heat recovery factor is 12.4%. With a power plant capacity of 5 Mw installed, the total area for extracting recoverable heat within the projected lifetime of a fracture surface of  $1.58 \times 10^6 \text{ m}^2$  was determined. The total mass flow rate of water injected into the large fracture was 57 kg/s. The discussion shows the ability of the model to estimate heat production and reservoir scale.

**Keywords:** enhanced geothermal system (EGS); hot dry rock (HDR); single fracture; heat production; reservoir design



**Citation:** Su, Z.; Zhai, H. Heat Production from Single Fracture Hot Dry Rock, Applications for EGS Reservoir Design. *Geotechnics* **2022**, *2*, 191–208. <https://doi.org/10.3390/geotechnics2010009>

Academic Editors: Yong Sheng and Kenneth Imo-Imo Israel Eshiet

Received: 9 December 2021

Accepted: 7 January 2022

Published: 23 February 2022

**Publisher's Note:** MDPI stays neutral with regard to jurisdictional claims in published maps and institutional affiliations.



**Copyright:** © 2022 by the authors. Licensee MDPI, Basel, Switzerland. This article is an open access article distributed under the terms and conditions of the Creative Commons Attribution (CC BY) license (<https://creativecommons.org/licenses/by/4.0/>).

## 1. Introduction

The amount of geothermal energy is enormous. Using geothermal energy can contribute to reducing greenhouse gas emissions and fossil energy use. Exploiting this renewable resource, however, is currently limited to hydrothermal systems in which naturally present fracture networks permit fluid circulation, allowing geothermal heat to be produced by tapping these hot fluids. Due to the exhaustibility of hot water, however, natural fluids are incapable of sustaining power plants at an economical level in the long term. A significantly small fraction of the Earth's geothermal potential has been developed so far, and an accelerated use of geothermal energy from deep hot dry rock (HDR) in the deep crust is feasible in the near future.

Deep hot rocks usually have limited permeability and low natural fluid content. Engineered or Enhanced Geothermal Systems (EGS) are the most effective methods for extracting geothermal energy from deep HDR. A body of hot rock is hydraulically fractured to become a geothermal reservoir to circulate and produce heat. Thus, the technique has been applied to extract geothermal energy from hot rocks by (1) creating permeability through hydraulic stimulation to activate existing rock fractures or creating new ones and (2) setting up and maintaining fluid circulation through these fracture networks by means of an injection system and production boreholes, allowing thermal energy to be transmitted to the land surface for human use. The project at Fenton Hill in north-central New Mexico, which began in 1974, was the first attempt to make a deep, full-scale EGS reservoir. Sequential EGS field experiments were conducted worldwide, and ongoing work is taking place in the Hunter Valley, Coso, Desert Peak, and Cooper Basin projects.

Previous attempts to develop EGS have proven that it is feasible to extract energy from the HDR through circulating water in the fracture network [1,2]. A high-performance EGS

requires a large reservoir with vast fractures for heat exchange, a sufficient water flow rate, and low water loss [3]. The fractures often have vertical planes that are perpendicular to the minimum principal stress in the horizontal planes. They may be intersected by natural joints or fractures and thus form a complicated network reservoir framework, as shown in Figure 1 [4]. The framework and water flow have been approximately determined through static pressurization testing and tracer technologies [1,3,5,6]. Regarding the uncertainty, the EGS reservoir framework is conceptualized as independent-multiple fractures connecting injection and production wells for fluid circulation [4]. The small fractures arising from natural joints are excluded from the simplified EGS reservoir framework (Figure 1).

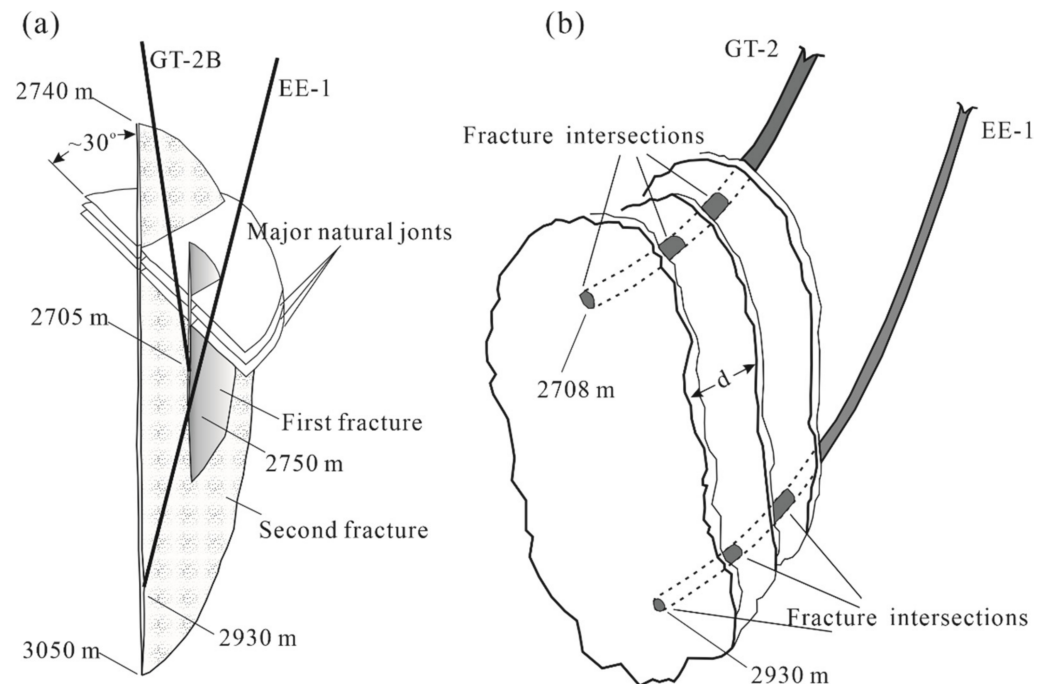


**Figure 1.** Framework of EGS fractured reservoir at the Fenton Hill field site (Dash et al., 1983). (a) referred reservoir geometry of EGS used to illustrate complicated network of fractures framework; (b) concept of reservoir geometry used to represent independent-multiple-fractures model.

A few studies have numerically investigated the performance of EGS reservoirs to predict heat production potential and thermal lifetime [7–10]. These studies have analyzed the couplings between hydrology (flow), heat transfer, rock mechanics, and chemistry [11,12]. Coupled multiphase fluid flow, heat transfer, and deformation in fractured porous rock was analyzed using a modeling approach [13]. A multiple interacting continua (MINC) method that is applicable to the numerical simulation of heat and multiphase fluid flow in multidimensional, fractured porous media was presented [7]. The stimulated volume was separated by fractures [9], and the matrix blocks were sometimes assumed to be impermeable and enclosed by orthogonal fracture sets with constant spacing [10].

It has been suggested that thermal-hydraulic coupling effects may have major effects on EGS reservoir performance [1,14]. Some studies have primarily focused on the coupling between hydrology and heat transfer in fractures [15,16]. Analytical solutions to study fluid flow and heat flow consider heat transfer between the matrix and fracture through a source/sink term. Only conductive heat transfer is considered for both the matrix and the fracture, while convective heat transfer through fractures is ignored [16,17]. Although the temperature of the fracture surface will rapidly decrease, the fluid is unable to harness any further heat from the fracture surface when flow channeling occurs [18,19]. These studies have assumed that the fluid temperature always equals the rock temperature; however, some studies have suggested that an evident temperature gradient exists between host rocks and circulating fluids [5,20,21]. Heat transfer coefficients, which typically depend

on the thermal properties of rock, as well as circulating fluid and its velocity [22], have been considered in heat transfer models. In each of these comprehensive works, heat extraction and temperature loss were evaluated using relatively complicated models or reservoir-scale systems that could not theoretically account for the effects of fluid flow in fractures on heat exchange and production through modeling. In this paper, the EGS reservoir framework is envisioned as independent-multiple fractures connecting injection and production wells. We propose a single fracture model based on further simplifying the concept of the independent-multiple-fracture reservoir to reveal thermal-hydraulic coupling in EGS reservoirs and the resulting heat production. The reservoir is represented by single fractures with homogeneous features and fluid flow during operation, and a unit fracture is defined as having extendibility to a larger surface area for heat extraction. A new analytical solution for the 1-D steady state conductive heat flow equation in a body of hot rock is derived, with some presumptions. The analytical solution is verified using a finite element solution and is then applied to present the temperature loss, heat production, and fracture scale of a reservoir.

## 2. Conceptual Model

The geometry of the structure was studied to understand the heat extraction process [16,23–26]. The complicated framework was reasonably characterized as independent multiple fractures for simplicity [4,16]. Some studies have suggested that the single fracture model is capable of capturing the basic characteristics and heat extraction process of EGS [26]. Fluid flow may follow an intricate path in the fracture network, but it undoubtedly goes from the injection well to the production well, and the produced energy is conclusively extracted from both sides of the hot fracture. The single fracture can be considered a set of jointed fractures along a tortuous flow path that are straightened to a single straight fracture. A single fracture behaves similarly to a jointed fracture for heat extraction and production. An EGS reservoir can be conceptually described as a single fracture with a vast surface area for heat transfer and recovery (Figure 2).

The conceptual model of a fractured reservoir is established on the basis of the previous works [16] and is shown in Figure 2. The fracture reservoir is composed of a rock matrix and independent multiple fractures (Figure 2a). The fluid in Figure 2a flows from the bottom of the fracture to the top, which is similar to how the fluid in Figure 1b flows from the deep borehole EE-1 along the fracture to the top borehole GT-2. The fracture width  $d$  in Figure 1b is denoted as  $\delta$  in Figure 2a. The fracture length is symbolized as  $l$ . The fracture height of  $\Delta y$  is unified (1 m) and extendable in the  $y$ -coordinate, allowing a vast fracture to be obtained. As previously explained, the single fracture system only includes one fracture in the body of the rock (Figure 2b). The original HDR temperature is  $T_{ro}$ . The injected water temperature is  $T_{f0}$ . Water is injected into the erected fractures and is circulated at a constant speed of  $u_f$ , and it is then heated by the hot rock to a high temperature,  $T_{fp}$ , at the outlet. The heat energy is abstracted by the circulating fluid from both walls of the fracture. In the 2-D coordinate system, the  $x$ -axis indicates the distance to the fracture, while the  $z$ -axis parallel to the water flow indicates the distance to the water inlet. The water inlet is designated as point  $(0, 0)$ . The water outlet is  $(0, l)$ . Heat conductively transfers toward the rock and water interfaces.

To make the problem simple and processable, we assumed the following about fluid flow in fractured rock: (1) the rocks are homogeneous blocks without the inclusion of pore fluids; (2) the two rock blocks have symmetrical changes in heat transfer and temperature loss relative to the mid fracture; (3) the transient water temperature is homogeneous at any specific fluid flow intersection in the fracture because of the small fracture width; (4) water is always liquid in the system; (5) the impact of temperature change on the thermo-physical properties of the system is ignored; and (6) the effect of thermal radiation is not considered [27].

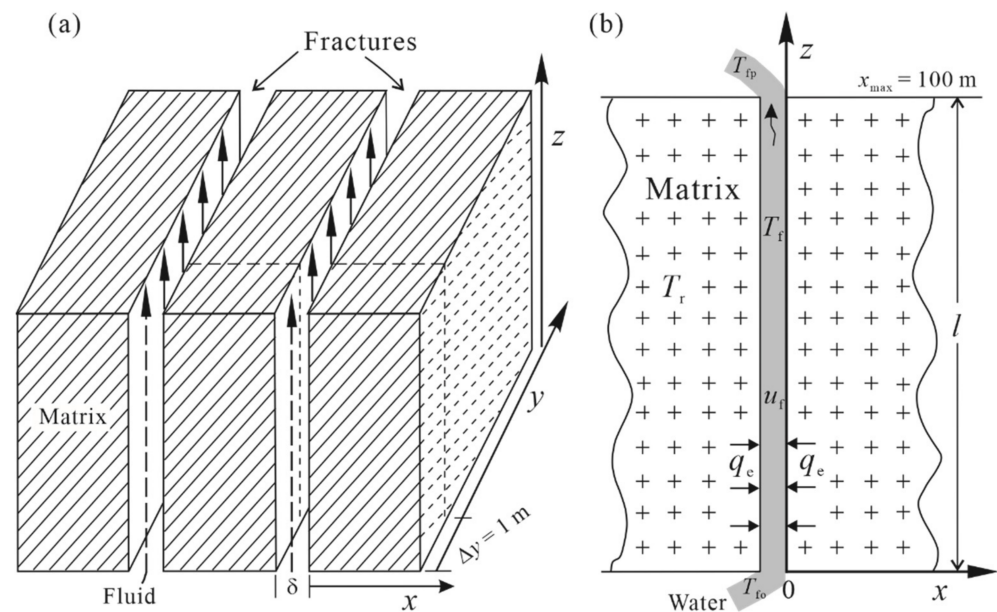


**Figure 2.** Conceptual model of EGS fracture reservoir. (a) A 3-D view of the independent-multiple-fracture model (Fox et al., 2013); (b) a 2-D view of the single-fracture EGS reservoir. The fracture height is  $l$  in  $z$  direction, and the fracture width is  $\delta$ . The fracture length is extendable in the  $y$  direction, and the unit fracture length of  $\Delta y$  ( $=1 \text{ m}$ ) will be used in following modeling.  $T_r$  denotes the rock temperature,  $T_f$  denotes the water temperature,  $u_f$  is the water flow rate,  $T_{f0}$  is the temperature of the injected water. Water is injected into the single fracture and is heated during circulation.  $q_e$  is the heat flow to the water from the rock, and  $T_{fp}$  denotes the temperature of the produced water.

### 3. Mathematical Models

In this paper, the EGS reservoir is conceptually envisioned as a single fracture system. Water is injected into a single fracture to extract geothermal energy from the hot rock, releasing heat that can then be utilized. Thus, the mathematical model concerning heat recovery and reservoirs contains temperature field and heat production equations. Conventional solutions governing the temperature equation are derived from both analytical and numerical methods with respect to the temperature distribution of the simplified model. Heat production can be computed by the changes in the water temperature via the fracture. The power plant capacity is used to determine the total heat production rate and the total fracture surface for heat exchange, both of which are used equally when designing EGS reservoirs.

#### 3.1. An Approximate Solution

To reach an analytical solution for water–rock temperature change, the following are assumed: (1) The thermal resistance at the water–rock interface is ignored. The heat exchange between hot rock and water at the interface is assumed to be an equilibrium process. The water temperature in the fracture equals the surface temperature of the fracture. The reasonability of this assumption has been confirmed in many practical cases [16,24,25,27]. (2) Heat conduction in the rock matrix along the  $z$  direction (parallel to water flow) is neglected for simplicity. The thermal conductivity in the rock matrix along the  $x$  direction (perpendicular to water flow) is included in the derivation of the analytical solution. (3) The effect of heat conduction in water is not considered in the model. The temperature change of the fluid in the fracture is determined exclusively by thermal convection and heat extraction. This assumption is based on the fact that the fluid is focused in a very narrow fracture.

According to heat transfer theory and approximation, it is apparent that the controlling fluid temperature equation in the fracture contains an unsteady term, convection term, and

source term and that the controlling equation for the rock temperature field only contains unsteady and heat conduction items. During the equation derivation process, the system temperature is defined as  $T$ , and the variables and parameters in the equations related to rock and fluid are specified with the subscripts  $r$  and  $f$ . The temperature field of rock can be expressed as a function of  $x$ ,  $z$ , and  $t$ , and the temperature of the work fluid in the fracture can be written as a function of  $z$  and  $t$ . Table 1 lists all of the parameters and properties used in the model.

**Table 1.** Reference values of parameters and properties used in the modeling.

Symbol	Definition	Value
$T_{ro}$	Original rock temperature (°C)	200
$l$	Length of fracture (m)	1000
$\Delta y$	Unit height of fracture (m)	1
$\rho_r$	Rock density (kg/m <sup>3</sup> )	2820
$c_r$	Heat capacity of rock (J/kg °C)	1170
$k_r$	Heat conductivity of rock (W/m °K)	2.8
$T_{f0}$	Temperature of injected water (°C)	30
$\rho_f$	Water density (kg/m <sup>3</sup> )	900
$c_f$	Heat capacity of fluid (J/kg °C)	4200
$h$	Heat transfer coefficient (W/m <sup>2</sup> K)	900
$\delta$	fracture width (mm)	2
$u_f$	Fluid flow rate (cm/s)	2

The water density is estimated as 900 kg/m<sup>3</sup> according to the water temperature produced at the Fenton Hill field site [1,4]. The rock temperature of the system is controlled by 1-D heat conduction [7,26]. The governing equation for rock temperature is:

$$\begin{cases} \frac{\rho_r c_r}{k_r} \cdot \frac{\partial T}{\partial t} - \frac{\partial^2 T}{\partial x^2} = 0 \\ T_{x=0} = T_f = T(0, z, t) \\ T_{t=0} = T_{ro} \end{cases} \quad (1)$$

where  $\rho_r$  is the rock density,  $c_r$  is the specific heat capacity of the rock, and  $t$  is the system operation time. The boundary condition for the differential equation is that the surface temperature of the fracture,  $T_{x=0}$ , equals the fluid temperature in the fracture,  $T_f$ . The initial rock temperature condition,  $T_{t=0}$ , is expressed as the original rock temperature,  $T_{ro}$ .

The fluid temperature of the system is controlled by heat convection along the fracture and heat extraction from two sides of the fracture [7]. The governing equation for the fluid temperature is as follows:

$$\begin{cases} \frac{\partial T}{\partial t} + u_f \cdot \frac{\partial T}{\partial z} = \frac{2q_e}{\rho_f c_f \delta} \\ q_e = k_r \cdot \frac{\partial T}{\partial x} |_{x=0} \\ T_{z=0} = T_{f0} \\ T_{t=0} = T_{ro} \end{cases} \quad (2)$$

where  $\rho_f$  is the fluid density,  $c_f$  is the fluid specific heat capacity, and  $k_r$  is the thermal conductivity of rock.  $q_e$  is the amount of heat transfer from hot rock to fluid and is represented as the amount of 1-D heat conduction perpendicular to the fluid flow at any fracture interface ( $x = 0$ ). It reflects the coupling of rock and fluid in the system. The boundary condition,  $T_{z=0}$ , is the temperature at the fracture entrance and is equal to the temperature of the injected fluid,  $T_{f0}$ . The initial condition,  $T_{t=0}$ , is equal to the original rock temperature,  $T_{ro}$ .

The solution for the above equations is derived using the Laplace transform method. This method uses the Laplace transform to convert the original heat equation into an ordinary differential equation that is more readily solved. The solution for the transformed

problem must then be inverted to obtain the solution to the original problem. Using the Laplace transform yields the transformed coupling equations:

$$\begin{cases} \frac{\rho_r c_r}{k_r} \cdot (s\bar{T} - T_{ro}) - \frac{\partial^2 \bar{T}}{\partial x^2} = 0 \\ \bar{T}_{x=0} = T(0, z, s) \\ \bar{T}_{s=0} = \frac{1}{s} \cdot T_{ro} \end{cases} \quad (3)$$

$$\begin{cases} s\bar{T} - T_{ro} + u_f \cdot \frac{\partial \bar{T}}{\partial z} = \frac{2k_r}{\rho_f c_f u_f \delta} \cdot \sqrt{\frac{s\rho_r c_r}{k_r}} \cdot \left(\frac{1}{s} \cdot T_{ro} - \bar{T}\right) \\ \bar{T}_{z=0} = \frac{1}{s} \cdot T_{f0} \\ \bar{T}_{s=0} = \frac{1}{s} \cdot T_{ro} \end{cases} \quad (4)$$

The Laplace transform is often interpreted as a transformation from the time domain, in which inputs and outputs are functions of time, to the frequency-domain, in which the same inputs and outputs are functions of complex angular frequency. The complex argument for  $s$  denotes the frequency domain. The transform turns the differential equations into polynomial equations, which are much easier to solve. After solving, using the inverse Laplace transform reverts to the time domain and yields the analytical solution for the temperature field.

The temperature of the rock matrix is calculated as follows:

$$T_r(x, z, t) = T_{ro} + (T_{f0} - T_{ro}) \cdot \operatorname{erfc} \left[ \frac{2k_r z + x\rho_f c_f u_f \delta}{2\rho_f c_f u_f \delta} \cdot \sqrt{\frac{\rho_r c_r u_f}{k_r \cdot (u_f t + z)}} \right] \quad (5)$$

The temperature of fluid in fracture is calculated as follows:

$$T_f(z, t) = T_{ro} + (T_{f0} - T_{ro}) \cdot \operatorname{erfc} \left[ \frac{k_r z}{\rho_f c_f u_f \delta} \cdot \sqrt{\frac{\rho_r c_r u_f}{k_r \cdot (u_f t + z)}} \right] \quad (6)$$

The analytical solution indicates that the temperatures of the rock matrix and fracture fluid are related to the original rock temperature, temperature of the injected fluid, the fracture width, the fluid flow rate, and the operation time. These analytical solutions for the temperature field are defined as Model 1 and are used to readily estimate heat production.

### 3.2. Finite Element Solutions

The analytical solution provides a potentially valuable framework for understanding the effects of heat conduction and exchange in a single fracture system, but its assumptions must be evaluated. For example, the method assumes that the heat conduction is perpendicular to the erected fracture over the history of operation time, vertical conductive heat is negligible, and heat exchange is an equilibrium process between the matrix and the fluid. The temperature distribution and heat extraction may be misestimated if the equilibrium heat change differs greatly from the kinetic heat exchange at the interface of the hot rock and from the circulation fluid in the system.

Thus, we used the standard finite element method to evaluate whether these assumptions are valid with varied fluid flow rates and fracture widths as well as to verify the applicability of the analytical method to EGS reservoir estimation. In this method, heat conduction in the rock matrix is solved in two dimensions. The heat exchange between the hot rock and the fluid is expressed as a kinetic process. The governing equations of the temperature field are:

$$\begin{cases} \frac{\rho_r c_r}{k_r} \cdot \frac{\partial T_r}{\partial t} - \frac{\partial^2 T_r}{\partial x^2} - \frac{\partial^2 T_r}{\partial z^2} + q_e = 0 \\ \frac{\partial T_f}{\partial t} + u_f \cdot \frac{\partial T_f}{\partial z} - \frac{2q_e}{\rho_f c_f \delta} = 0 \\ q_e = ha(T_{r,x=0} - T_f) \end{cases} \quad (7)$$

Here, conduction exclusively refers to heat transfer in the rock. It proceeds in two dimensions, perpendicular and parallel to the fracture, and is quantitatively determined by the temperature gradient in the system. The fluid flow temperature regime in the fracture is still determined by 1-D fluid convection and heat extraction from both surfaces of the fractures. The amount of heat transferred to fluid is expressed as a kinetic form,  $q_e = ha\Delta T$  [21], where  $h$  is the heat transfer coefficient,  $a$  is the surface area at one side of the fracture, and  $\Delta T$  is the temperature difference at the rock–fluid interface.

The differential equations for fluid flow and heat transfer can be resolved numerically with the initial and boundary conditions:

$$\begin{cases} T_{r,t=0} = T_{r0} \\ T_{f,t=0} = T_{r0} \\ T_{f,z=0} = T_{f0} \end{cases} \quad (8)$$

The conditions are the same as those used to derive the approximate solution; where the initial temperatures of the rock and fluid are taken as  $T_{r0}$ , and the fluid temperature at the entrance of the fracture is specified as  $T_{f0}$ . To confine the heat conduction to the boundaries of the rock block, the additional boundary conditions are:

$$\begin{cases} \frac{\partial T_r^-}{\partial z} \Big|_{z=0} = 0 \\ \frac{\partial T_r^+}{\partial z} \Big|_{z=l} = 0 \end{cases} \quad (9)$$

These additional conditions suggest that heat cannot transfer downwards at the lower boundary and upwards at the upper boundary. The finite element solution of the temperature field is defined as Model 2 and will be used to verify the validity of Model 1 derived in this paper.

### 3.3. Fracture Reservoir Design

Focused fluid flow extracts heat from the hot rock and releases it after being produced at production boreholes. The heat production depends on the fluid output and temperature. For the single fracture EGS reservoir, the heat production in a unit time is as follows:

$$q_p = \rho_f u_f \delta c_{pf} (T_{fp} - T_{f0}) \quad (10)$$

where  $q_p$  is the heat production and  $T_{fp}$  is the produced fluid temperature and is equal to  $T_f(l, t)$ . By integrating the heat production rate within the entire duration of production, the total amount of heat production can be then written as:

$$Q_p = \int_0^t q_p dt = \rho_f u_f \delta c_{pf} \int_0^t (T_{fp} - T_{f0}) dt \quad (11)$$

A commercially operated EGS plant needs sufficient fluid circulation and high-temperature production. The total fracture surface area must match the project requirement of the geothermal power plant. The total fracture surface for heat exchange should be generally estimated before fracturing hot rock and installing power equipment. This value can be determined by the relationship between heat production and thermoelectric conversion. The correlation is:

$$H_p = \bar{Q}_p \frac{A}{l} = \frac{1}{t} \frac{A}{l} Q_p \quad (12)$$

Here,  $H_p$  is the heat production efficiency for economical electricity generation.  $\bar{Q}_p$  is the average heat production of the unit fracture over time,  $\bar{Q}_p = Q_p/t$ . The unit fracture surface area can be obtained by multiplying the fracture length,  $l$ , and by the unit fracture height,  $\Delta y$ , which thus equals  $l \times \Delta y = l$ . The unit fracture surface area equals  $l \times \Delta y = l$ .

$A$  is the total fracture surface area required to sustain efficient heat production and power plant operation.

The total fracture surface area can be also related to the total injection rate of the work fluid if the fracture is flooded by the fluid flow. A low injection rate may incur incomplete rock–fluid interactions and heat extraction because the fluid may bypass the partial fracture surface. For a specific fracture size and fluid flow rate, the injected rate of circulation fluid  $A$  can be theoretically determined as follows:

$$M_f = m_f \frac{A}{l} = \rho_f \delta u_f \frac{A}{l} \quad (13)$$

where  $M_f$  is the total injection rate of work fluid with respect to the fracture size,  $A$  and  $l$ , and  $m_f$  is the mass flux of the fluid bypassing the unit fracture,  $m_f = \rho_f \delta u_f$ .

#### 4. Calculation Results

EGS reservoirs are usually developed in deep hot dry rocks. The temperature field of the reservoir is influenced by the original rock temperature, fracture size, and fluid injection. These parameters also impact heat extraction efficiency and the reservoir lifespan. The parameters and properties in the calculations refer to the values published in a previous study [21] and are listed in Table 1.

##### 4.1. Validity of Model 1

The analytical solution for the water–rock temperature field is derived based on idealized presumptions. The foremost presumption is the 1-D heat conduction perpendicular to fracture/water flow (Figure 2); the temperature evolution may be very different from that obtained by Model 2. Thus, the applicability of Model 1 should be validated before it is used to study the temperature field, water–rock interaction, heat production, and reservoir performance.

Figure 3 compares the fluid temperature along the fracture. The fluid temperature in the fractures is alternately calculated by Models 1 and 2 at different water flow rates and fracture widths and is compared at the intervals of 1 month, 1 year, and 3 years. Here, the fracture length is specified as 200 m, and the original rock temperature is 200 °C. The water temperature curves in Figure 3a are delineated at a low water flow rate of 0.5 cm/s and a small fracture width of 0.5 mm.

The water temperature calculated by Model 1 is generally higher than that calculated by Model 2. The temperature difference is as high as 41 °C at  $t = 1$  month and  $z = 5$  m and decreases with time. The water temperatures have similar features at high water flow fluxes, and the largest temperature differences appear at  $t = 1$  month. However, the difference becomes smaller at the higher water flow rates (Figure 3b–d). The temperature differences were 25 °C at  $u_f = 0.5$  cm/s and  $\delta = 1$  mm (Figure 3b), 13 °C at  $u_f = 1$  cm/s and  $\delta = 1$  mm (Figure 3c), and 8 °C at  $u_f = 2$  cm/s and  $\delta = 1$  mm (Figure 3d). The flow path length with the largest difference occurred at  $z = 10$  m,  $z = 20$  m, and  $z = 40$  m, respectively. Therefore, the fluid temperature difference decreased as the water flow rate and operation time increased.

Figure 4 shows fluid temperatures in the fracture at specific points of the flow path. The two kinds of fluid temperatures are calculated by Models 1 and 2 at different water flow rates and fracture widths. Compared to at the  $z$  values (flow path length), the water temperatures illustrate the temperature evolution trend and the differences between the two calculations.

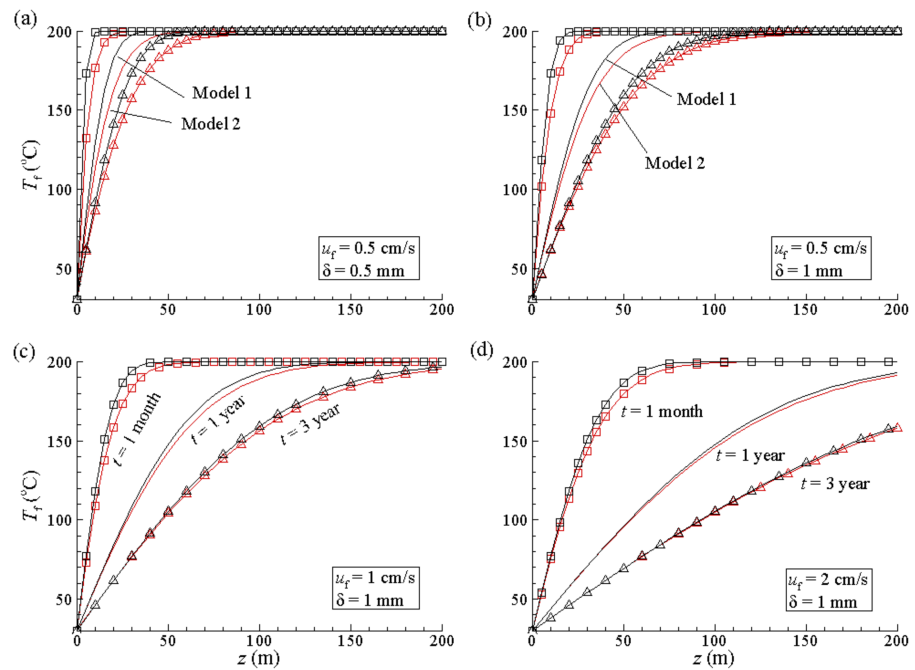


**Figure 3.** Comparison of water temperature along the fracture. The water temperature in the fracture is alternately calculated by Model 1 and Model 2 at different water flow rates and fracture widths and is compared at the operation times of 1 month, 1 year, and 3 years. The difference between the two fluid temperatures becomes smaller as the water flow rate and operation time increase. The temperature is calculated at (a)  $u_f = 0.5 \text{ cm/s}$  and  $\delta = 0.5 \text{ mm}$ , (b)  $u_f = 0.5 \text{ cm/s}$  and  $\delta = 1 \text{ mm}$ , (c)  $u_f = 1 \text{ cm/s}$  and  $\delta = 1 \text{ mm}$ , and (d)  $u_f = 2 \text{ cm/s}$  and  $\delta = 1 \text{ mm}$ .

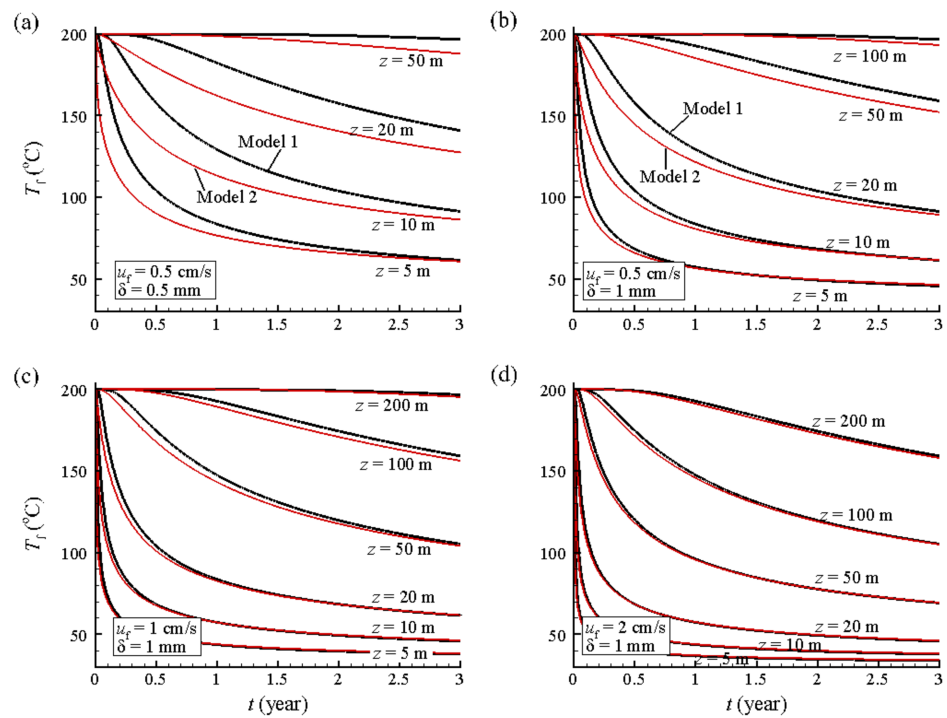


**Figure 4.** Comparisons of water temperatures calculated by Model 1 and Model 2 at the different water flow rates and fracture widths. The temperatures are compared at the specific points along the fracture. The time duration is 3 years. (a–d) The difference between the two fluid temperatures becomes smaller with time and is lowered at high water flow flux.

The temperature curves in Figure 4a are calculated at a water flow rate of 0.5 cm/s and at a fracture width of 0.5 mm and indicate a large temperature difference at different  $z$  values. The water temperatures calculated by Model 1 are greater than those calculated by Model 2, and the temperature difference decreases at higher  $z$  values. The temperature difference was as high as 44 °C at  $z = 5$  m and  $t = 17$  days and 30 °C at  $z = 10$  m and  $t = 78$  days and fell to 20 °C at  $z = 20$  m and  $t = 1$  year. Figure 4 also shows that the temperature difference decreases and even disappears with time at high  $z$  values.

The temperature difference completely disappears at the high water flow rate and the enhanced fracture width (Figure 5), suggesting that the analytical model is applicable for the evaluation of fluid flow and heat extraction in the single fracture system. The values of  $u_f = 2$  cm/s and  $\delta = 2$  mm are used as the reference conditions in the following model.

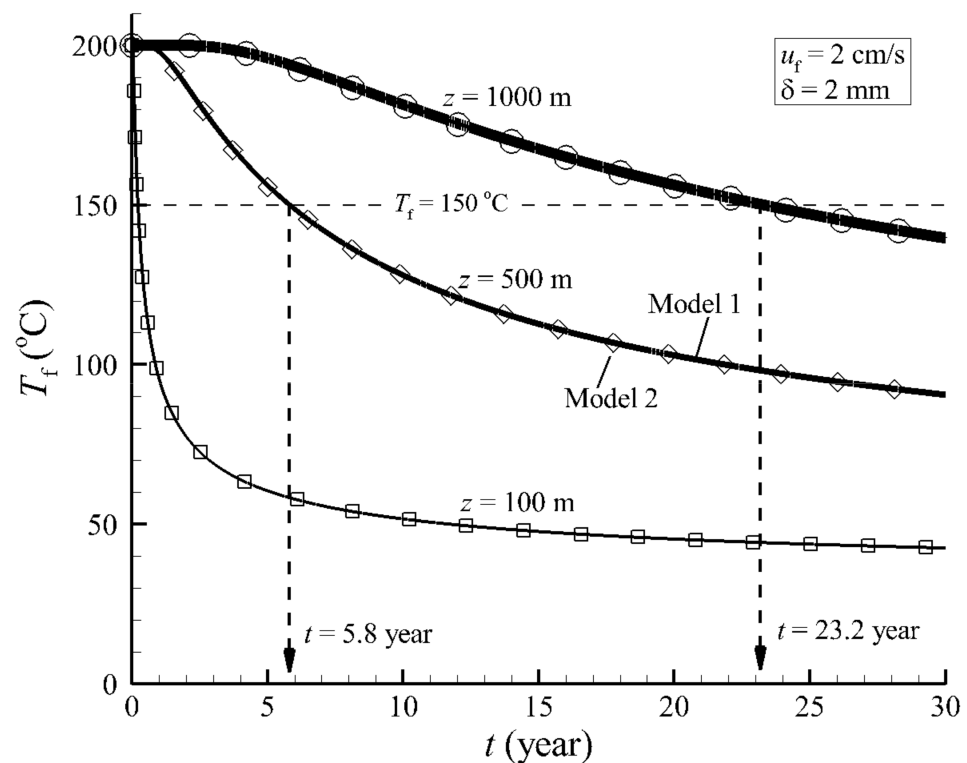


**Figure 5.** Comparisons of fluid temperatures at specific  $z$  values. The fluid temperatures are calculated by Model 1 (solid line) and Model 2 (markers) at the water flow rate of 2 cm/s and the fracture width of 2 mm and are compared at the  $z$  values of 100 m, 500 m, and 1000 m. The temperature difference does not appear in the 30 years duration of operation.

#### 4.2. Temperature Field

Model 1 was validated by Model 2 and can therefore be used to trace the temperature evolution of rocks. Figure 6 shows the temperature evolution of the rock at the defined reference conditions over a period of 30 years in the simulation domain ( $x \leq 100$  m and  $z \leq 1000$  m). The temperature pattern is unique because of the heat conduction type and invariable water flow. These include the following: (1) the cold zone at the water inlet, (2) the heat extraction front proceeding as a hypotenuse of a right-angled triangle, and (3) the evolution of a symmetrical low-temperature zone along the fracture.

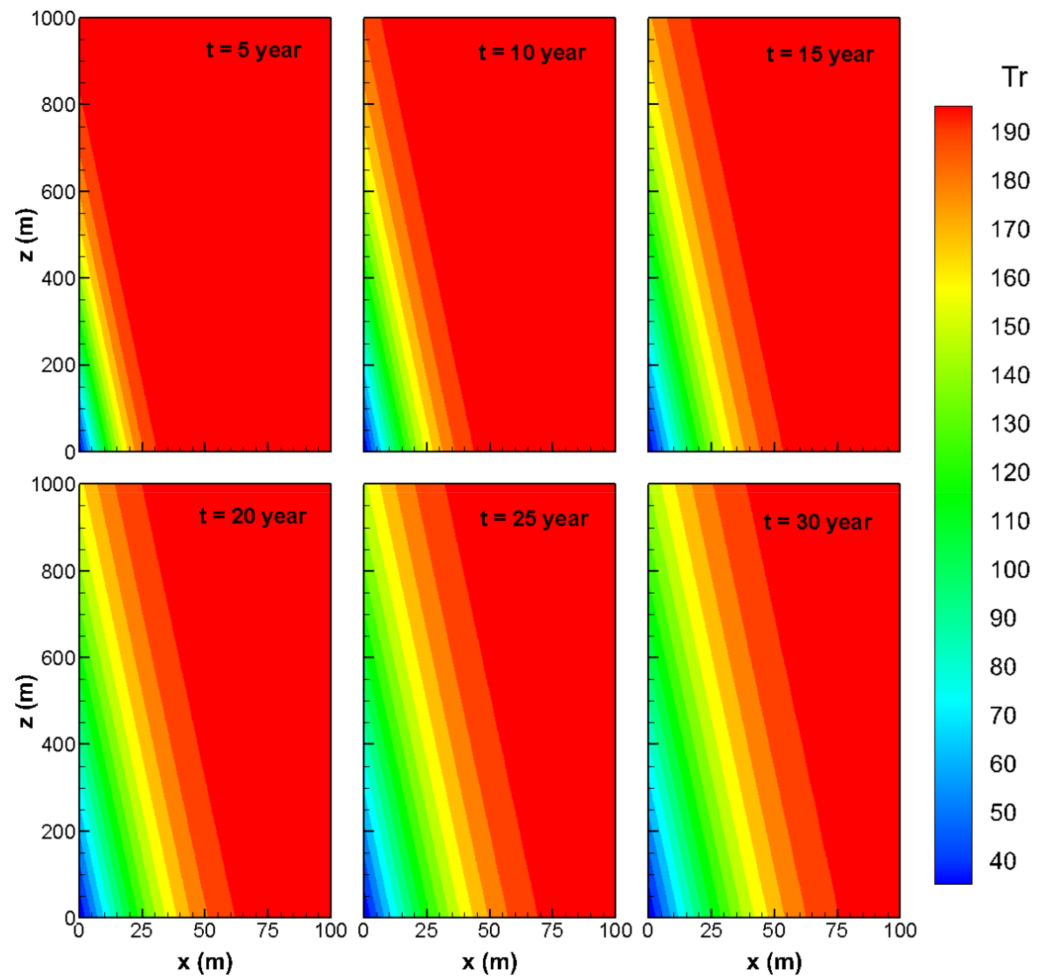


**Figure 6.** Evolution of the rock temperature during the heat mining process under the reference conditions. The temperature distribution timing is 5 years, 10 years, 15 years, 20 years, 25 years, and 30 years.

Cold zones in the rock are caused by the injection of cold water into the fracture. Here, the heat conduction is quicker, and heat extraction proceeds remarkably at the zone. The fracture temperature further away from the cold zone approaches the original temperature because the water flow is heated in the fracture and because the temperature gradient at the interface is relatively small. Therefore, the low temperature zone forms a right-angle triangle, and its evolution is controlled by the 1-D heat conduction of Model 1.

EGS was developed to extract geothermal energy from hot rocks by circulating water through man-made fractures. Water temperature and its evolution are the crucial factors for evaluating heat extraction efficiency and EGS reservoir potential. Figure 7 shows the water temperature distribution along the fracture at the reference conditions over time. The water temperature along the flow path is enumerated at the operation times of 5, 10, 15, 20, 25, and 30 years, respectively. The temperature increases with a water flow path of  $z$  and an injected water temperature of  $30\text{ }^{\circ}\text{C}$ , suggesting that water flow is heated by hot rock. The heating intensity decreases with time, resulting in reduced temperatures. The declining water temperature is consistent with the reduction in the rock temperature gradient and heat conduction rate.

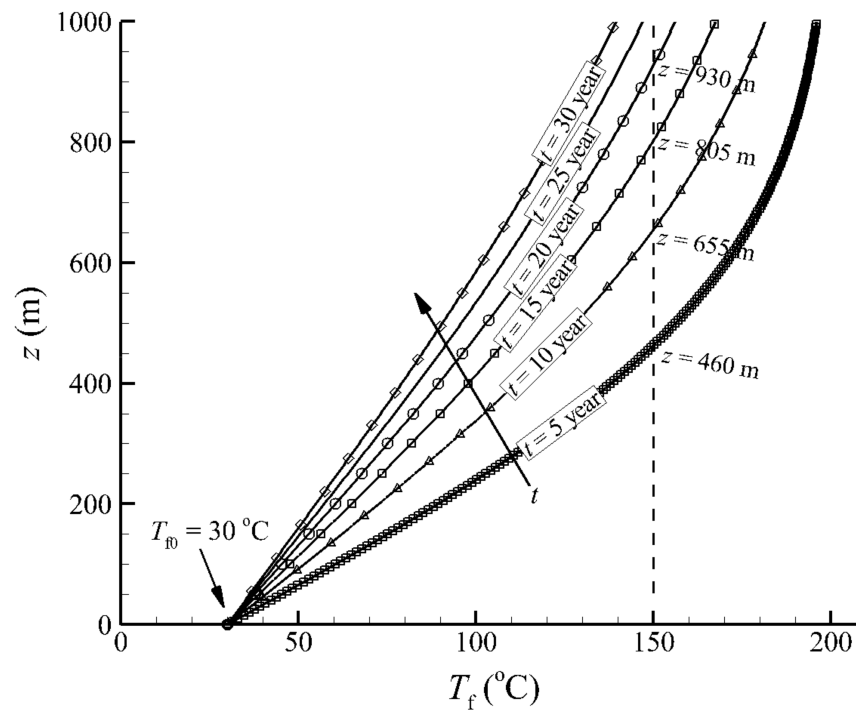


**Figure 7.** Temperature evolution of water flow in the fracture at the reference conditions. The water temperature regime is calculated at the times of 5 years, 10 years, 15 years, 20 years, 25 years, and 30 years, respectively.

4.3. Temperature of Produced Water

The aim of EGS development is to produce sufficient amounts of hot water from geothermal reservoirs. Thus, the temperature of the produced water is the first index for evaluating heat production efficiency and EGS reservoir lifespan. If a water temperature of 150 °C is considered the criterion for acceptable industrial utilization on the earth surface, the needed fracture length for water circulation must be extended with the production time (Figure 7). The lifespan of a single fracture reservoir is 10 years if the fracture length is 460 m and 20 years if the fracture length is 930 m.

The analytical fluid temperature solution makes it clear that the produced water temperature at the fracture outlet is a function of the injected water temperature, water flow rate and fracture width, and production time. Figure 8 shows the effect of the injected water temperature on the produced water temperature at the reference conditions for rock, fractures, and water flow. The produced water temperature generally decreases with the production time and can be elevated by increasing the temperature of the injected water. The injected water temperatures were 30, 40, 50, and 60 °C, respectively. The produced water temperature fell to approximately 140 °C after a production duration of 30 years when the injected water was at the reference temperature. It increased to 150 °C when the injected water temperature was 60 °C. For the temperature criterion of produced water (150 °C), the acceptable production duration is set as 23.2 years at the reference  $T_{f0}$ , and approaches 30 years when  $T_{f0} = 60$  °C.

The parameter pair of the water flow rate and fracture width indicates water flow flux through the fracture. A high value of  $u_f \delta$  implies that more water is heated in the fracture. The water may not be sufficiently heated when it arrives at the outlet. Figure 9 shows the effect of injected water flow flux (equivalent to  $u_f \delta$ ) on the produced water temperature. The temperature of the produced water can be elevated by lowering the water flow flux. It is 189 °C at the smaller flux and 109 °C at the higher flux after a production duration of 30 years. Meanwhile, water flow rates have the same effects on the performance of the produced water temperature as the fracture width. For example, the produced water temperature at the  $u_f = 1$  cm/s and  $\delta = 2$  mm (solid line) pair is the same as that at the  $u_f =$

2 cm/s and  $\delta = 1$  mm (markers) pair. At this high water flux, the single fracture reservoir has a 10.3 year lifespan.

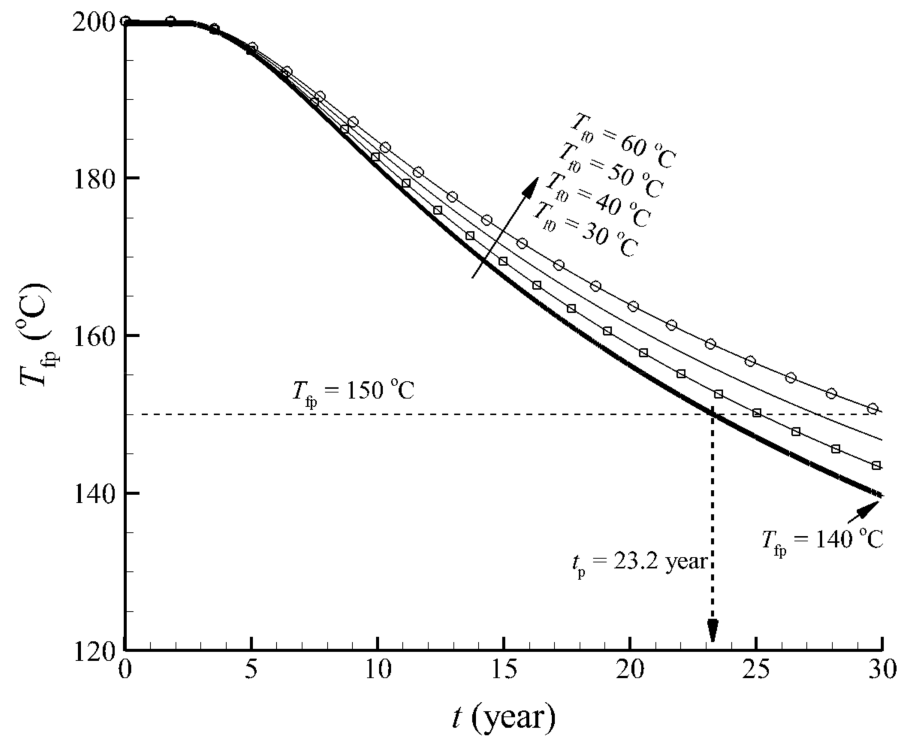


**Figure 8.** Effect of injected water temperature on produced water temperature at the reference conditions of rock, fractures, and water flow. The injected water temperature is 30 °C, 40 °C, 50 °C, and 60 °C, respectively.

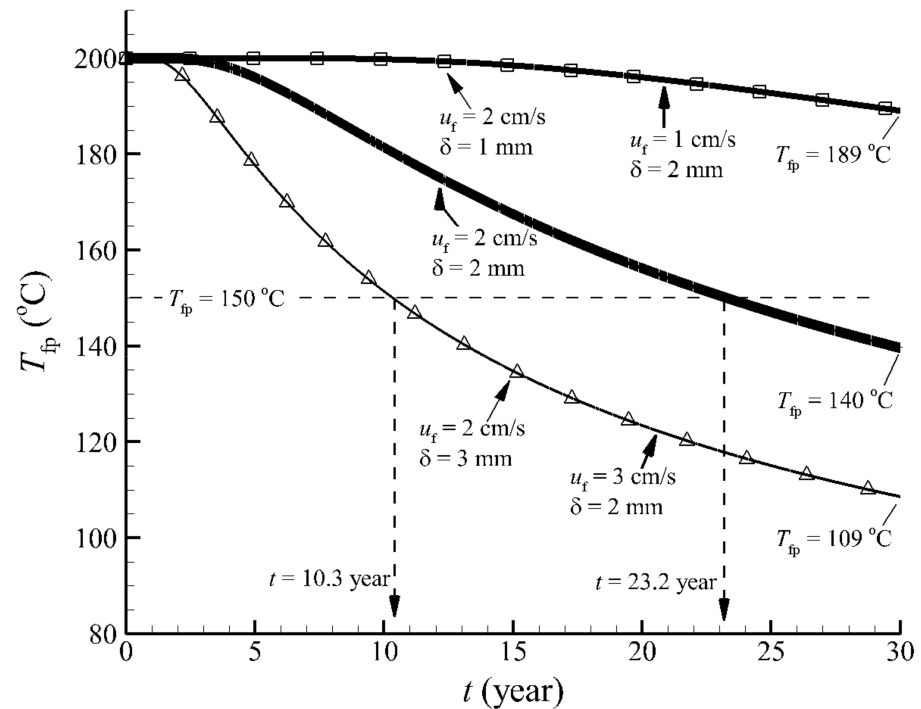


**Figure 9.** Effect of injected water flow flux on produced water temperature. The production water temperature is reduced at the high water flux. The water flow rate has the same effect on the produced water temperature as the fracture width.

#### 4.4. Heat Production

A good EGS reservoir is able to sustain high production levels of heated water over a planned amount of time. Figure 10 shows heat production from the single fracture reservoir at the reference conditions. The temperature of the produced water decreases with the operation time. The fractured system can maintain the production of high temperature water (above 150 °C) for 23.2 years (Figure 10a), which is indicated as the projected lifetime of an EGS reservoir with the given conditions. The reduction in the temperature of the produced water incurs a decrease in the heat production rate  $q_p$  with time. The average heat production rate  $\bar{q}_p$  is 22.2 kw above the reservoir lifetime of 23.2 years (Figure 10b). The accumulative heat production over the reservoir lifetime is  $16.3 \times 10^{12}$  J (Figure 10c) and the heat recovery factor is 12.4% (Figure 10d).

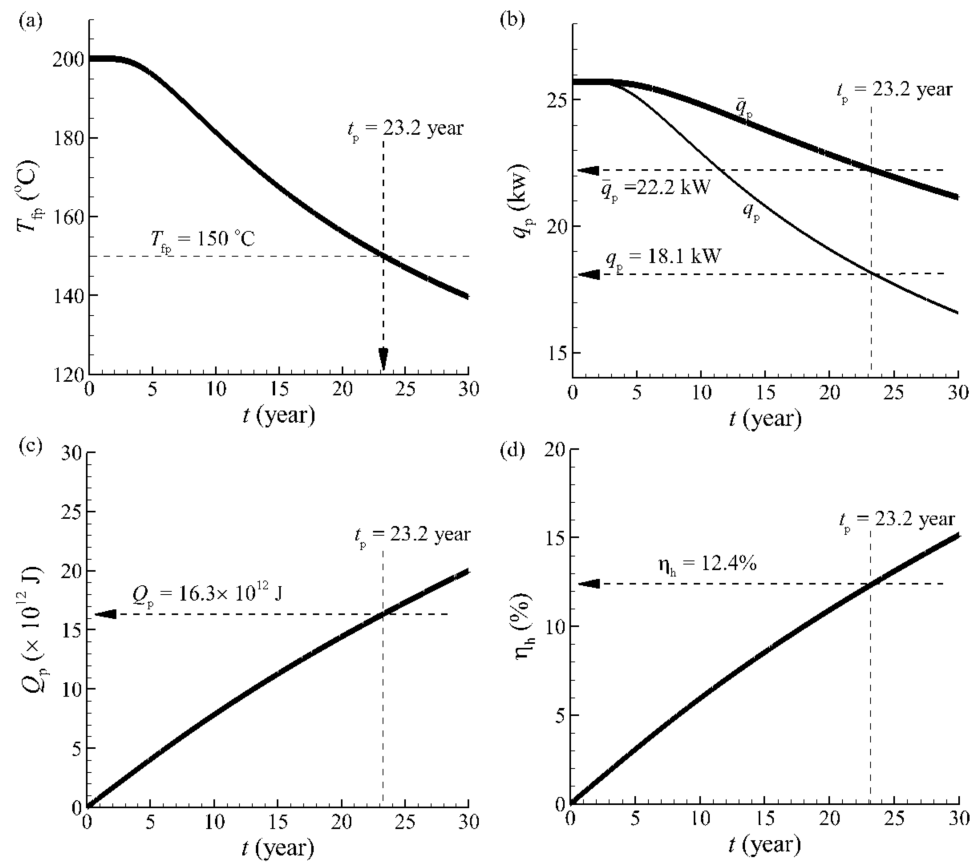


**Figure 10.** Heat production from the single fracture reservoir at the reference conditions. (a) Temperature of produced water; (b) heat production rate with time and average heat production rate over time; (c) cumulative heat production over time; (d) heat recovery factor with time.

EGS development aims to effectively generate electricity using deep geothermal energy. The working fluid, water, is heated by hot rock as it circulates through the fractured rock. A sufficient fracture surface for heat transfer is necessary for an industrial EGS power plant. Thus, many fractures or a fracture network is usually constructed by hydraulic fracturing or other methods to assure that the massive amounts of water flow are heated. The fracture surface illustrated in the conceptual model can be expanded to large quantities to reflect the massive heat exchange and production at the reservoir scale.

Figure 11 shows the relationships between the total area of the fracture surface and heat production, electric generation, and water injection. The electricity power is calculated assuming 15% heat to electric-power efficiency. As Equation (12) indicates, the heat production increases proportionally with the fracture surface area (Figure 11a). If a plant with a 5 MW capacity is to be installed, a minimum fracture surface area of  $1.58 \times 10^6$  m<sup>2</sup> must be

prepared to sustain stable operations for 23.2 years (Figure 11b). The total geothermal energy of 31.6 PJ will be produced over the projected production duration (Figure 11a). Meanwhile, the total mass flow rate of water according to Equation (13) is 57 kg/s (Figure 11c). As noted here, the calculation is based on the reference conditions of hot rock, fracture size, and water flow. However, the predication techniques can be readily used to design fracture reservoirs.

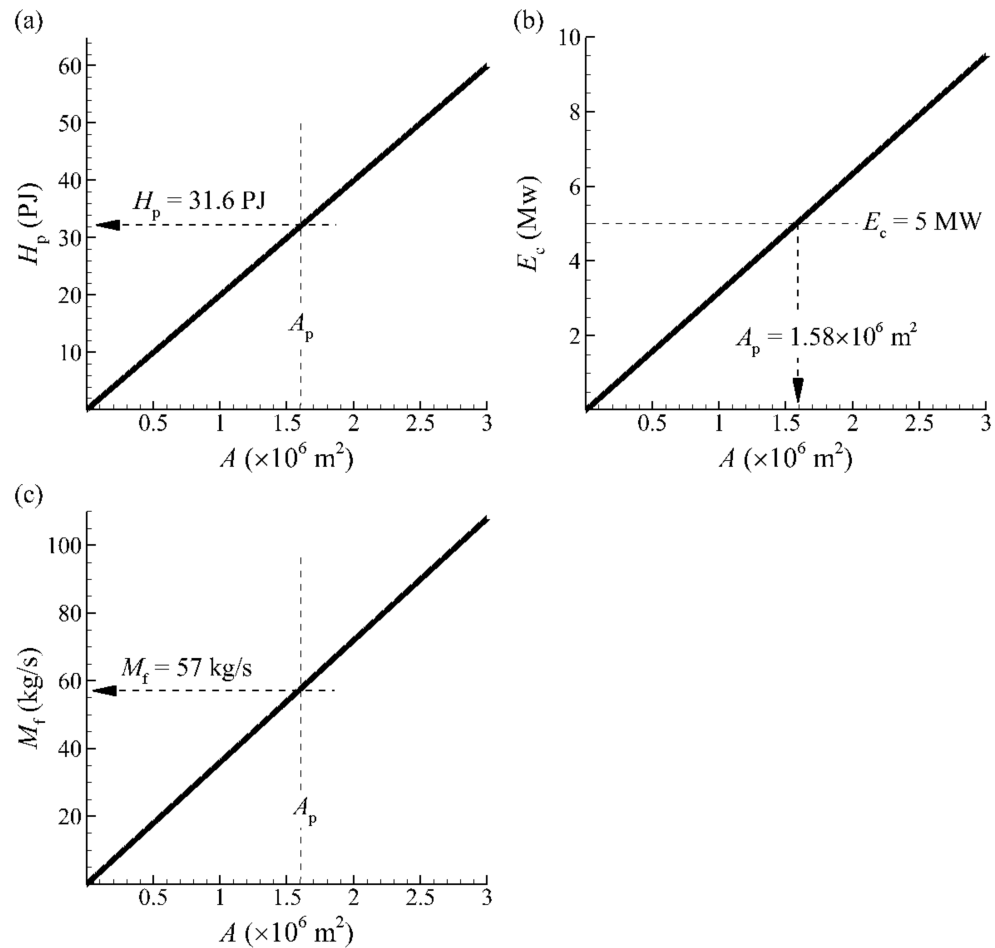


**Figure 11.** Change in total heat production, electric generation, and water injection rate with the expandable area of fracture surface of EGS reservoir. (a) Heat production; (b) electricity generation; (c) total injection rate of water.

**5. Discussion**

We verified our simplified model and calculations in three ways. First, the single fracture model was a conceptual simplification of an EGS reservoir and could be expanded to a complicated network of fractures. Second, the agreement between the analytical model and numerical calculation at fast flow rates and long terms was able to verify both the model and its calculation. Third, the heat production and reservoir design calculations are similar to the predication made by previous researchers. The calculations are adequately convergent for the conclusions drawn in this paper.

We assumed an impermeable rock matrix, and fluid leak-off from the fracture to the matrix was not considered. In fact, the effect of fluid leak-off was found to be relatively small. Because the HDR object developed by EGS is deep and dense bedrock, the amount of porous fluid is very small due to the limited porosity and permeability. In the very early stage, high-temperature fluid can be produced from the rock relatively quickly because of the big pressure difference between the rock mass and fractures and can significantly affect the fluid temperature in fractures. However, with the release of pore pressure, the

pore fluid activity will inevitably decrease, and the influence on the fracture fluid will be significantly reduced [28].

Fracture growth can be followed by microseismic event monitoring during stimulation and fluid circulation in an EGS reservoir. The fractures generally grow vertically, in a direction determined by the stress field, although they may be altered by early joints and other structures. The reservoir performs as a complicated network of fractures but can be simply represented as multiple independent fractures in the body of hot rock [4,16]. The reservoir is connected by two wells for water injection and production that define the length of the independent fractures (Figure 1). The single fracture model is used to quantify the thermal-hydraulic characteristics of one fracture (Figure 2). However, the single fracture is extendable in the height direction ( $y$ -coordinate) and can thus represent the total fracture surface of multiple fractures as well as the thermal effect. Therefore, it is reasonable to study the complicated geothermal reservoir by the simplified single fracture system model.

In this paper, the analytical model is used to represent fluid flow and temperature distribution in the fracture and in the hot rock body. The approximate temperature field solution was based on the presumption of 1D heat conduction perpendicular to the fracture and equilibrium heat transfer at the water–rock interface. The model was checked using the finite element model with water temperature prediction in the fracture. The numerical model contained 2-D heat conduction in the rock body and kinetic heat transfer between the rock and the water [21]. The water temperature predicted by the analytical model was higher than that calculated by the numerical model at low water flux (or  $u_f \delta$ ) and during the early operation stages. The similarity between the comparisons suggests that the analytical model is feasible for predicting reservoir heat production at fast flow rates over long-term operation.

The fracture aperture is assumed to be a constant during the lifespan of the EGS reservoir. However, it is highly sensitive to pore pressure changes and drops in temperature. The increase in the fracture aperture means that the fluid flux increases under fixed production pressure conditions, and more working fluid exchanges heat with the fracture surfaces. Thus, the heat exchange efficiency and heat output are reduced [26,29]. The purpose of deep geothermal energy production is to generate electricity by converting heat to electricity. The heat production rate is constrained by the planned plant capacity. Heat production can be obtained through quantities of outlet water flux and water temperature. The project lifetime of a fracture reservoir is associated with the lowermost water temperature for electricity generation and is substantially determined by fracture size and water flow. It can be prolonged by lowering the water flux, but the fracture surface area from heat exchange must be enlarged to match rated heat production and electricity generation. At the reference conditions of fracture size and water flow rate, a minimum fracture surface area of  $1.58 \times 10^6 \text{ m}^2$  must be prepared to sustain the stable operation of a plant with a 5 Mw capacity for 23.2 years. The total mass flow rate of water is 57 kg/s. Total geothermal energy of 31.6 PJ will be recovered, with 12.4% of the total thermal energy being a recoverable fraction. The data suggest that a small portion of geothermal energy can be produced economically; a smart strategy must be developed to improve heat recovery.

The calculations in this paper are based on the fracture rock and fluid properties and the utilizable temperature and heat–electric conversion parameters. Other factors that significantly affect the system calculations include fracture morphology, natural fluids in rock, variable viscosity and fluid density, the short circuiting of fluid between injection and production wells, and water loss to the surrounding rock during reservoir operation; however, our calculations provide a good reference to predict the heat production, recovery, and design of the geothermal reservoir.

Although the analytical equation solution of hot and dry rock temperature is two-dimensional, it can fully reflect the heat transfer and temperature change in the three-dimensional space of hot rock mass. Other improvements needed in the model include the modelling of reservoir elasticity, thermoelasticity, and poroelasticity, leading to a frac-

ture fluid pressure, temperature, and reservoir compliance-dependent fracture aperture width [26,29]. Work in these directions is under development.

## 6. Conclusions

In this paper, we presented a new analytical solution for a 1-D steady state conductive heat flow equation in the body of hot rock that includes perpendicular water flow in the single fracture and the equilibrium heat transfer from rock to water. We also presented a finite element 2-D solution for the conductively dominated temperature equation that includes perpendicular water flow and kinetic heat exchange between materials. Arithmetic equations were also derived to demonstrate heat production from the hot rock via water flow in the idealized single fracture and to design geothermal reservoirs by the calculations. The applicability of the analytical solution is verified by the numerical solution and is limited to the conditions of fast water flow rates or high water flux and long fluid pathways. For commercial utilization, the EGS reservoir lifespan is limited by the temperature of the produced water. The power plant capacity requires the total heat production rate from the geothermal reservoir and the total fracture surface area to extract the recoverable heat within the projected reservoir lifetime. The mathematical simulations use both analytical and numerical methods to show the ability of conductively dominated EGS reservoirs to recover thermal energy and to estimate heat production and reservoir scale. With such modular methods operating successfully and flexibly, one can access heat production and EGS reservoir potential. Some factors, however, such as fracture morphology, natural hot water, and variable water viscosity and density, will require consideration in subsequent papers.

**Author Contributions:** Conceptualization, Z.S. and H.Z.; methodology, Z.S.; validation, Z.S.; formal analysis, Z.S.; investigation, H.Z.; writing—original draft preparation, H.Z.; writing—review and editing, Z.S.; project administration, Z.S.; funding acquisition, Z.S. All authors have read and agreed to the published version of the manuscript.

**Funding:** This work was financially supported by the National High-tech R&D PROGRAM (863 PROGRAM) (2012AA052802) and the Guangzhou Institute of Energy Conversion, the Chinese Academy of Sciences (y107a41001).

**Institutional Review Board Statement:** Not applicable.

**Informed Consent Statement:** Not applicable.

**Data Availability Statement:** Not applicable.

**Acknowledgments:** The authors acknowledge the technical support given by Nengyou Wu and Lihua Liu during the development of the research program.

**Conflicts of Interest:** The authors declare no conflict of interest.

## References

1. Brown, D.W.; Duchane, D.V. Scientific progress on the Fenton Hill HDR project since 1983. *Geothermics* **1999**, *28*, 591–601. [[CrossRef](#)]
2. Genter, A.; Evans, K.; Cuenot, N.; Fritsch, D.; Sanjuan, B. Contribution of the exploration of deep crystalline fractured reservoir of Soultz to the knowledge of enhanced geothermal systems (EGS). *Comptes Rendus Geosci.* **2010**, *342*, 502–516. [[CrossRef](#)]
3. Tester, J.W.; Anderson, B.J.; Batchelor, A.S.; Blackwell, D.D.; DiPippo, R.; Drake, E.M.; Garnish, J.; Livesay, B.; Moore, M.C.; Nichols, K.; et al. *The Future of Geothermal Energy*; Technical Report. DOE Contract DE-AC07-05ID14517; Massachusetts Institute of Technology: Cambridge, MA, USA, 2006.
4. Dash, Z.V.; Murphy, H.D.; Aamodt, R.L.; Aguilar, R.G.; Brown, D.W.; Counce, D.A.; Fisher, H.N.; Grigsby, C.O.; Keppler, H.; Laughlin, A.W.; et al. Hot Dry Rock Geothermal Reservoir Testing- 1978 to 1980. *J. Volcanol. Geotherm. Res.* **1983**, *15*, 59–99. [[CrossRef](#)]
5. Wu, Y.-S.; Pruess, K. Numerical simulation of non-isothermal multiphase tracer transport in heterogeneous fractured porous media. *Adv. Water Resour.* **2000**, *23*, 699–723. [[CrossRef](#)]
6. Pruess, K. Numerical simulation of multiphase tracer transport in fractured geothermal reservoirs. *Geothermics* **2002**, *31*, 475–499. [[CrossRef](#)]
7. Pruess, K.; Narasimhan, T.N. A practical method for modeling fluid and heat flow in fractured porous media. *Soc. Pet. Eng. J.* **1985**, *25*, 14–26. [[CrossRef](#)]

8. Xu, T.; Pruess, K. Numerical simulation of injectivity effects of mineral scaling and clay swelling in a fractured geothermal reservoir. *Geotherm. Resour. Council Trans.* **2004**, *28*, 269–276.
9. Sanyal, S.K.; Butler, S.J. An analysis of power generation prospects from enhanced geothermal systems. In Proceedings of the World Geothermal Congress 2005, Antalya, Turkey, 24–29 April 2005.
10. Pruess, K. Enhanced geothermal systems (EGS) using CO<sub>2</sub> as working fluid—A novel approach for generating renewable energy with simultaneous sequestration of carbon. *Geothermics* **2006**, *35*, 351–367. [[CrossRef](#)]
11. Taron, J.; Elsworth, D. Thermal–hydrologic–mechanical–chemical processes in the evolution of engineered geothermal reservoirs. *Int. J. Rock Mech. Min. Sci.* **2009**, *46*, 855–864. [[CrossRef](#)]
12. Taron, J.; Elsworth, D.; Min, K.-B. Numerical simulation of thermal-hydrologic-mechanical-chemical processes in deformable, fractured porous media. *Int. J. Rock Mech. Min. Sci.* **2009**, *46*, 842–854. [[CrossRef](#)]
13. Rutqvist, J.; Wu, Y.-S.; Tsang, C.-F.; Bodvarsson, G. A modeling approach for analysis of coupled multiphase fluid flow, heat transfer, and deformation in fractured porous rock. *Int. J. Rock Mech. Min. Sci.* **2002**, *39*, 429–442. [[CrossRef](#)]
14. Hanano, M. Contribution of fractures to formation and production of geothermal resources. *Renew. Sustain. Energy Rev.* **2004**, *8*, 223–236. [[CrossRef](#)]
15. Jiang, F.; Luo, L.; Chen, J. A novel three-dimensional transient model for subsurface heat exchange in enhanced geothermal systems. *Int. Commun. Heat Mass Transf.* **2013**, *41*, 57–62. [[CrossRef](#)]
16. Fox, D.B.; Sutter, D.; Beckers, K.F.; Lukawski, M.Z.; Koch, D.L.; Anderson, B.J.; Tester, J.W. Sustainable heat farming: Modeling extraction and recovery in discretely fractured geothermal reservoirs. *Geothermics* **2013**, *46*, 42–54. [[CrossRef](#)]
17. Bai, M.; Roegiers, J.-C. Fluid flow and heat flow in deformable fractured porous media. *Int. J. Eng. Sci.* **1994**, *32*, 1615–1633. [[CrossRef](#)]
18. Bataillé, A.; Genthon, P.; Rabinowicz, M.; Fritz, B. Modeling the coupling between free and forced convection in a vertical permeable slot: Implications for the heat production of an Enhanced Geothermal System. *Geothermics* **2006**, *35*, 654–682. [[CrossRef](#)]
19. Ghassemi, A.; Kumar, G.S. Changes in fracture aperture and fluid pressure due to thermal stress and silica dissolution/precipitation induced by heat extraction from subsurface rocks. *Geothermics* **2007**, *36*, 115–140. [[CrossRef](#)]
20. Sanyal, S.K.; Granados, E.E.; Butler, S.J.; Horne, R.N. An Alternative and Modular Approach to Enhanced Geothermal Systems. In Proceedings of the World Geothermal Congress 2005, Antalya, Turkey, 24–29 April 2005.
21. Shaik, A.R.; Rahman, S.S.; Tran, N.H.; Tran, T. Numerical simulation of Fluid-Rock coupling heat transfer in naturally fractured geothermal system. *Appl. Therm. Eng.* **2011**, *31*, 1600–1606. [[CrossRef](#)]
22. Holman, J. *Heat Transfer*, 7th ed.; McGraw-Hill, Inc.: New York, NY, USA, 1990.
23. Gringarten, A.C.; Witherspoon, P.A.; Ohnishi, Y. Theory of heat extraction from fractured hot dry rock. *J. Geophys. Res.* **1975**, *80*, 1120–1124. [[CrossRef](#)]
24. McFarland, R.D.; Murphy, H.D. *Extracting Energy from Hydraulically Fractured Geothermal Reservoirs*; ASME: State Line, NV, USA, 1976.
25. Wunder, R.; Murphy, H. *Thermal Drawdown and Recovery of Singly and Multiply Fractured Hot Dry Rock Reservoirs*; Informal Report W-7405-ENG.36; Los Alamos Scientific Laboratory of the University of California: Los Alamos, NM, USA, 1978.
26. Cheng, A.H.-D.; Ghassemi, A.; Detournay, E. Integral equation solution of heat extraction from a fracture in hot dry rock. *Int. J. Numer. Anal. Methods Géoméch.* **2001**, *25*, 1327–1338. [[CrossRef](#)]
27. Tian, L. Experimental and Numerical Study on the Thermo-Hydrological Coupling of Fractured Rocks. Master’s Thesis, Beijing Jiao Tong University, Beijing, China, 2009. (In Chinese with English Abstract).
28. Fan, Z.; Parashar, R.; Jin, Z.H. Impact of convective cooling on pore pressure and stresses around a borehole subjected to a constant flux: Implications for hydraulic tests in an EGS reservoir. *Interpretation* **2020**, *8*, 1–31. [[CrossRef](#)]
29. Fan, Z.; Parashar, R. Analytical Solutions for a Wellbore Subjected to a Non-isothermal Fluid Flux: Implications for Optimizing Injection Rates, Fracture Reactivation, and EGS Hydraulic Stimulation. *Rock Mech. Rock Eng.* **2019**, *52*, 4715–4729. [[CrossRef](#)]